[EN-046] Study of INS-Aided GPS Tracking Performance under Simulated Ionospheric Scintillation Associated with Plasma Bubbles

(EIWAC 2010)

+T. Tsujii*, T. Fujiwara*, Y. Suganuma*, and K. Matsunaga**

*Aviation Program Group
Japan Aerospace Exploration Agency (JAXA)
Tokyo, Japan
[tsujii | fujiwara | suganuma]@chofu.jaxa.jp

**CNS Department
Electronic Navigation Research Institute (ENRI)
Tokyo, Japan
matunaga@enri.go.jp

Abstract: Robust tracking of GNSS signal in a harsh environment such as a severe ionospheric scintillation and intentional/unintentional interference is a challenge for civil aviation. The use of inertial sensor would improve the tracking performance since the Doppler frequency shift caused by aircraft dynamics could be compensated by the inertial measurements. Therefore, an INS-aided GPS tracking loop was developed and implemented in a software receiver. Since flight test data under scintillation was not available at this stage, the digital intermediate frequency data was simulated for the use of software receiver. The real data of scintillation associated with plasma bubble, which was observed at south Japan, was analyzed and extracted intensity/phase variation were embedded in the simulated DIF data. As a result of preliminary test, reduction of carrier phase error by Doppler aiding was observed though cycle slips occurred even with aiding.

Keywords: GPS Tracking Loop, Doppler Aiding, INS, Ionospheric Scintillation, Software Receiver

1. INTRODUCTION

Although GPS has been widely used for vehicle navigation, the reliability is not sufficient for aircraft operation and therefore some kinds of augmentation system are necessary. In Japan, a satellite based augmentation system, MSAS (MTSAT Satellite-based Augmentation System), which is compatible with the United States WAAS and the European EGNOS systems, has been developed by the Japan Civil Aviation Bureau, and has been operational for enroute and non-precision approach since September 2007[1]. Also, a prototype of GBAS for category-I precision approach has been developed by ENRI [2]. However, even with such augmentation systems, the availability might not be sufficient under a harsh environment such as a severe ionospheric scintillation and intentional/unintentional interference (Fig.1).

To retain carrier tracking is important for precision approach using GBAS, since carrier phase is used for smoothing pseudorange. If cycle slips occurred in several channels, the corresponding smoothing procedures have to be restarted, and would cause a missed approach. The use of inertial sensor would improve the tracking performance since the Doppler frequency shift caused by aircraft dynamics could be compensated by the inertial measurements. Therefore, Japan Aerospace Exploration Agency commenced research on INS-aided GPS tracking loop and developed prototype algorithms. Last year flight experiments were conducted in order to evaluate the aided loop where a navigation grade INS tightly-coupled with GPS as well as a low-cost MEMS INS loosely-coupled with GPS were installed to provide aiding information. Also, two GPS front end units with different clock (TCXO

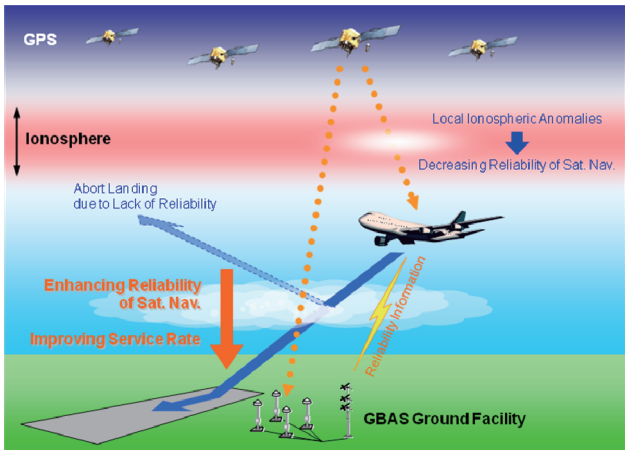

Figure 1 Degraded availability of precesion approach due to ionospheric anomalies (conceptual figure)

and OCXO) were installed to collect digitized IF data. Off-line analyses during aircraft take-off showed that the noise band width in tracking loop could be reduced to three hertz by aiding [3].

Since the basic aiding algorithms have been developed, demonstrations of the INS-aided GPS tracking loop performance under simulated ionosphere scintillation is the purpose at the next step. It is well known that the storm enhanced density (SED) associated with a severe magnetic storm is the major threat for GBAS. However, the effect of plasma bubble has to be considered in the countries at relatively low magnetic latitude including Japan since it is common phenomenon in such region and often causes scintillation as well as spatial gradient [4]. Therefore, the performance evaluation under ionosphere scintillation associated with plasma bubbles is aimed in this research.

A software receiver is used to develop the algorithms of tracking loop, which is not accessible in case of usual hardware GPS receivers. Also a software-based signal simulator is used to generate DIF (Digitized Intermediate Frequency) data which includes the scintillation effect associated with plasma bubble. A real scintillation data set collected by ENRI was used to extract the variation of carrier phase and amplitude due to the scintillation. A preliminary result of the signal tracking simulation using the generated data is shown in this paper.

2. DOPPLER AIDED TRACKING LOOP

2.1 Doppler Aiding for PLL

A simple Doppler aiding in phase lock loop has been developed for a preliminary test, and the effect of INS aiding is evaluated in this paper. The Doppler aided PLL model is shown in Fig. 2. Although third order loop filters are more robust than second order filters in high dynamics environments, they might be less stable and the transient response might be larger. Therefore, a second order loop filter was used as a prototype loop filter for all analyses hereafter.

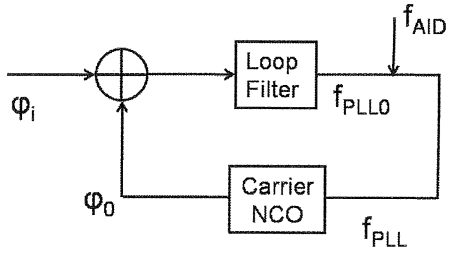

Figure 2 Doppler aided PLL model

The frequency of PLL is expressed as :

$$f_{PLL} = f_D + f_{clk} + f_{noise} \quad (1),$$

where f_D and f_{clk} are Doppler and clock frequency [5].

If the loop is aided, the frequency of PLL can be rewritten as:

$$f_{PLL} = f_{PLL0} + f_{AID} \quad (2)$$

Although three types of aiding frequency such as delta Doppler (Δf_D), Doppler (f_D), and Doppler and clock frequency ($f_D + f_{clk}$) are tested in the previous work[3], the Doppler frequency aiding is used in this paper.

The Doppler frequency is computed as follows:

$$f_D = \frac{\mathbf{e} \cdot (\mathbf{v}_S - \mathbf{v}_R)}{\lambda} \quad (3)$$

where $\mathbf{v}_S$, $\mathbf{v}_R$, $\mathbf{e}$, and λ are satellite velocity, receiver velocity ,line-of-sight unit vector, and L1 wave length, respectively.

The Doppler aiding algorithm is implemented in the iPRx software receiver developed by iP-solutions Inc. The receiver can be seen as consisted of two major components. One is an USB front end, which has functions to receive L1 GPS signal, down-convert it and digitize. The digitized signal is repacked and decimated if required and sent to PC through a USB. The sampling rate is 16 mega samples per second. The software component of the receiver includes baseband processing and navigation processing parts. The base band processor includes acquisition and tracking modules, and the phase locked loop (PLL) of this software receiver was modified by JAXA for this work. The DIF data obtained by front end during flight tests were processed in off-line mode by the software receiver, and the fundamental performance of INS aiding was demonstrated. On the other hand, the simulated DIF data including scintillation effect is processed in this paper.

2.2 Effect of Doppler Aiding Under Scintillation

Theoretical performance of Doppler aiding is described in this section. Fig. 3 shows the carrier phase error (1 σ) vs. noise bandwidth of the second order PLL where scintillation is not included. The aircraft acceleration (0.15g) is included and this effect is assumed to be removed by Doppler aiding. The empirical tracking threshold (15 degrees) is shown by dashed red line while the tracking margins with/without aiding are shown by arrows. It can be seen that the phase error is generally reduced by Doppler aiding. However, a rather wider bandwidth (e.g. 20 Hz) can guarantee stable tracking even without aiding. Next, the carrier error under a strong scintillation (S4=0.95 , T=7.1e-3(rad^2/Hz), p=2.5) is shown in Fig. 4. where S4 is an index for amplitude scintillation while T, and p are parameters for phase scintillation (see section 3). The phase errors caused by

amplitude/phase scintillation are computed by equations as follows [6,7];

$$\sigma_{\delta\phi,scin\_therm}^{\ 2} = \frac{B_n}{C/N_0}\cdot\frac{1}{1-S4^2}\left(1+\frac{1}{2\eta C/N_0(1-2\cdot S4^2)}\right) \quad (4)$$

$$\sigma_{\delta\phi,scin\_phase}^{\ 2} = \frac{\pi T}{2 f_n^{p-1}\sin([p-1]\pi/4)} \quad (5)$$

where $B_n(=3\pi f_n/2\sqrt{2})$ is noise bandwidth of PLL and η is the pre-detection integration time (=0.001 sec in this paper). Comparing Fig. 3 and Fig. 4, the phase error is greatly increased due to the scintillation. However, Doppler aiding could give some tracking margin and the rate of cycle slip would be smaller than the case without aiding.

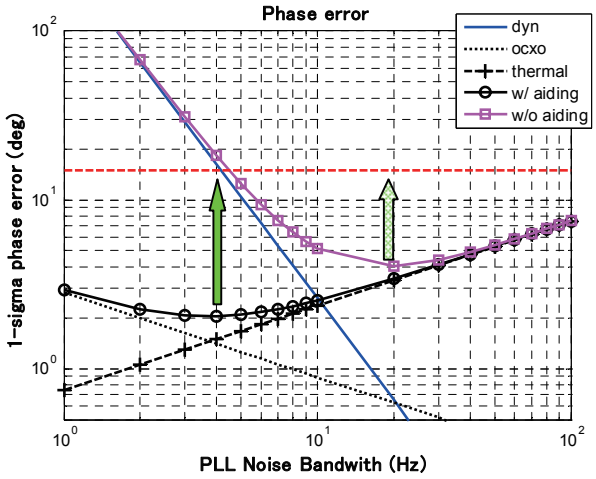

Figure 3 Phase error caused by several error sources (without scintillation)

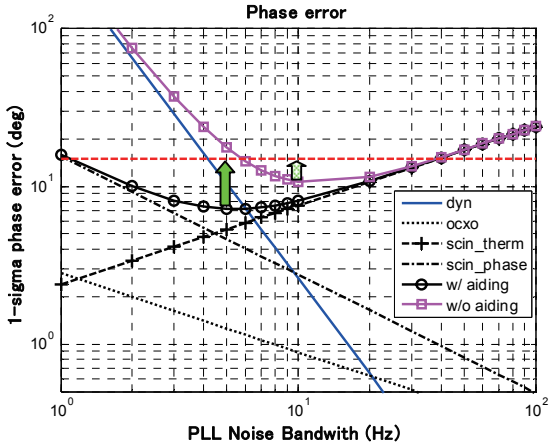

Figure 4 Phase error caused by several error sources (with scintillation)

3. SCINTILLATION WITH PLASMA BUBBLE

In order to simulate the scintillation associated with plasma bubble, observation data from GSV4004 are analyzed and the characteristics are extracted. The GSV4004 is designated for monitoring scintillation and gives scintillation related parameters as well as GPS pseudorange and carrier phase. Fig. 5 shows TEC (Total Electron Content) obtained at Naha (N26°13' 43, E127°40' 44), Japan, on April 14, 2004 (12:40 – 13:10, GPS time) [8]. The TEC for PRN 15 was varied with minimum at 12:59 (21:59, local time). Fig. 6 shows the trajectory of GPS satellites during the same period. The PRN 15 was seen west-southwest from Naha.

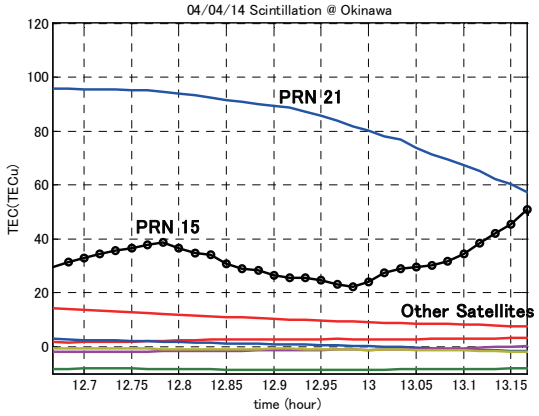

Figure 5 Variation of TEC at Naha (bias not calibrated)

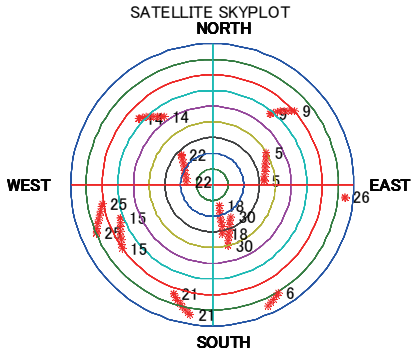

Figure 6 Trajectory of GPS satellites observed at Naha.

On the other hand, the TEC values observed at Taiwan by NICT (National Institute of Information and Communications Technology, Japan) is shown in Fig. 7. Rapid decrements and increments of TEC were seen at the approximately same time with Naha, and they seemed to be associated with plasma bubbles.

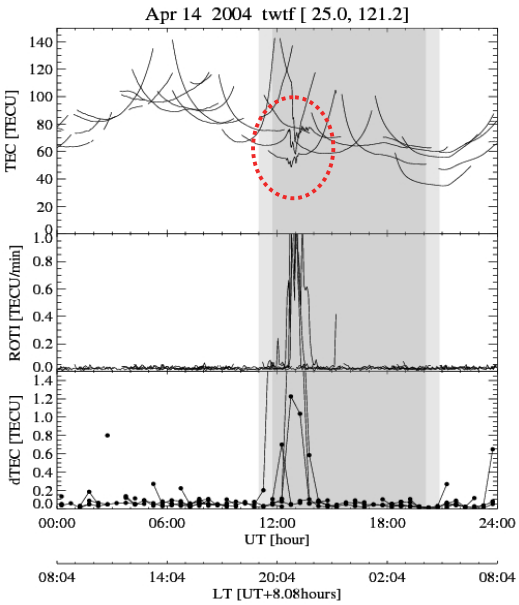

Figure 7 TEC variation observed at Taiwan.
(http://wdc.nict.go.jp/IONO2/TEC-ROTI/)

Next, the index of amplitude scintillation (S4) is shown in Fig. 8. S4 is defiend by Eq. 6 where I denotes the GPS signal intensity.

$$S4 = \sqrt{\frac{\langle I^2 \rangle - \langle I \rangle^2}{\langle I \rangle^2}} \qquad (6)$$

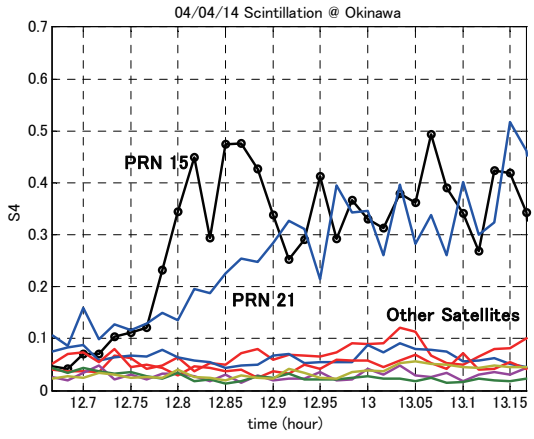

Figure 8 Variation of S4 index at Naha

The S4 for PRN increased and reached to 0.5. Though the S4 for PRN21 was large, it might be due to multipath error because the satellite elevation was low (see Fig. 6). In order to verify the source of S4 variation, the difference between pseudorange and carrier phase (Code Carrier Divergence, CCD) can be used since multipath error on pseudorange is much larger than that on carrier phase [9]. The CCD (1 σ) were plotted against S4 index for various satellites (Fig. 9). If the CCD was larger than 0.25, the intensity variation was considered as caused by multipath. Therefore, the large S4 index for PRN21 was due to multipath.

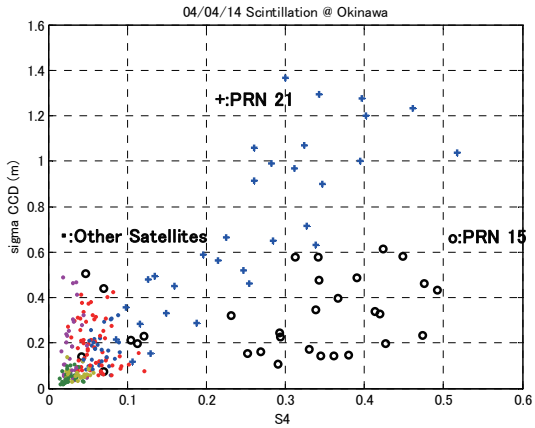

Figure 9 CCD (1 σ) vs. S4 index for various satellites

Then statistics of the residuals of detreanded carrier phase (σ_ϕ) for PRN15 and PRN21 are shown in Figure 10. The σ_ϕs were computed over 60 seconds and were plotted at every minute. The variation of σ_ϕ for PRN15 correlates with S4 index shown in Fig. 8, while there seems no scintillation effect on PRN21.

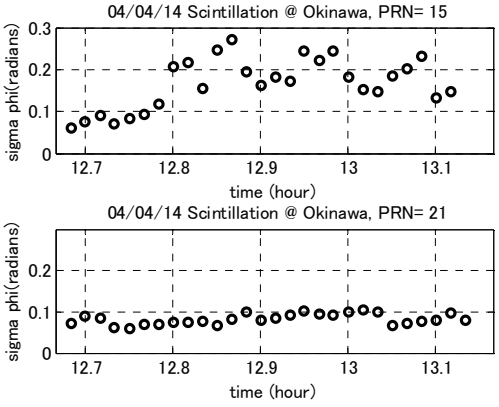

Figure 10 σ_ϕ for PRN15 (top) and PRN21 (bottom)

The power spectral densities of intensity and phase computed by using GSV4004 50Hz data at 12:51 (S4=0.48, σ_ϕ=0.25) are shown in Fig. 11 and Fig. 12 respectively.

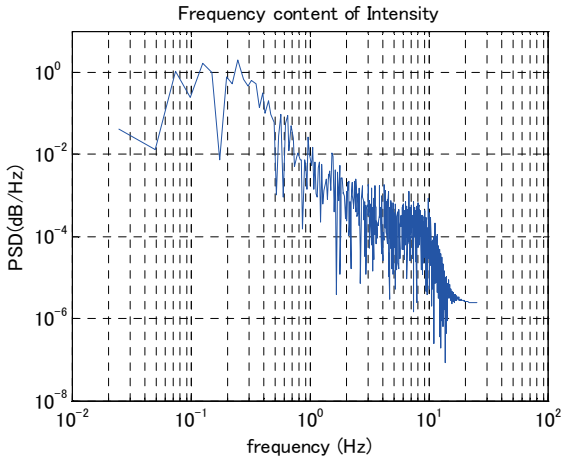

Figure 11 Intensity spectral density (12:51)

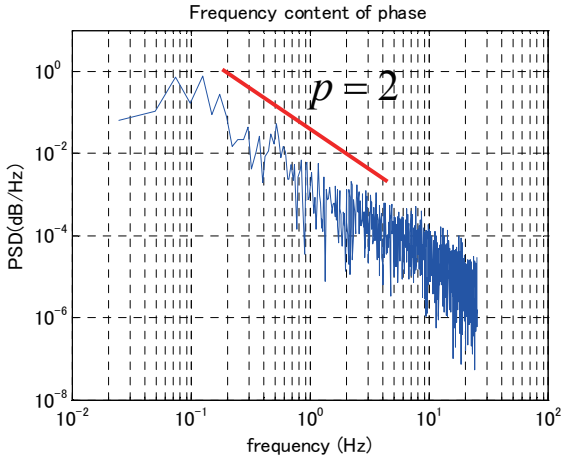

Figure 12 Phase spectral density (12:51)

It is known that the phase spectral density under scintllation is approximated as follows;

$$P_{\delta\phi}(f) = T \cdot f^{-p} \qquad (7),$$

where T is a strength parameter (rad^2/Hz) and p is a unitless slope parameter which is typically 2.0 – 3.0. The time series of intensity/phase variations (12:50 – 12:51), from which the spectral densities are computed, are shown in Fig. 13.

The power spectral density of intensity/phase and time series at the beginning of scintillation (12:42 - 12:43) are also shown in Fig.14-16 for references.

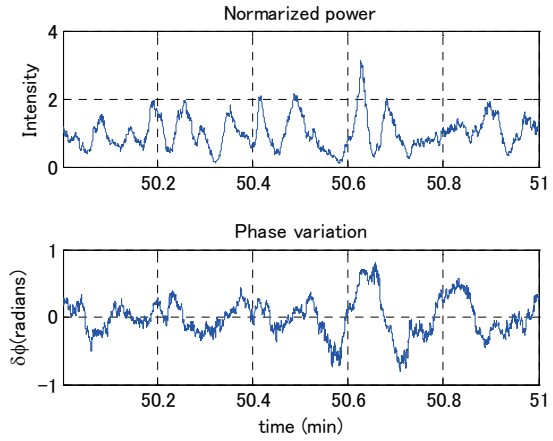

Figure 13 Normalized intensity and phase variation (12:50 - 12:51)

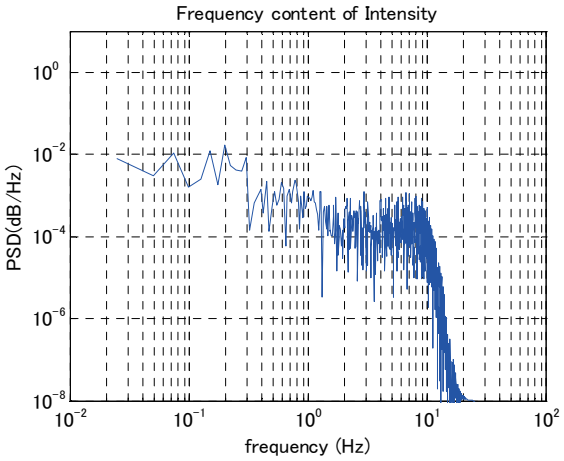

Figure 14 Intensity spectral density (12:43)

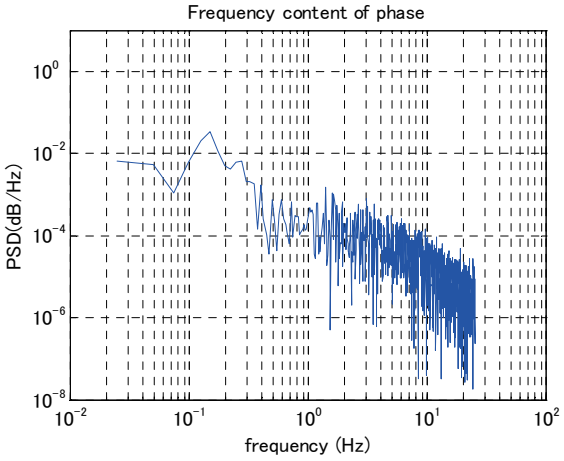

Figure 15 Phase spectral density (12:43)

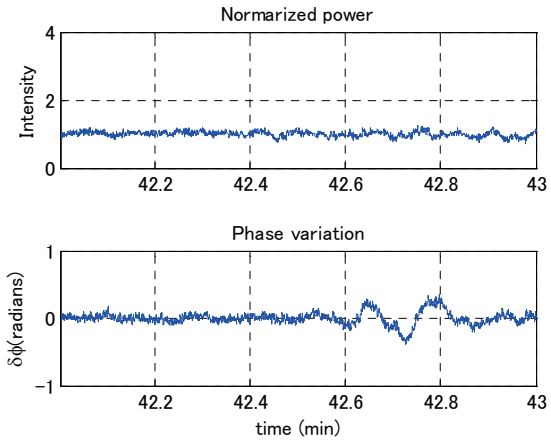

Figure 16 Normalized intensity and phase variation (12:42 - 12:43)

4. SIMULATION OF DOPPLER-AIDING UNDER SCINTILLATION

4.1 Simulation of Flight Profile and DIF data

In order to evaluate the performance of Doppler aiding implemented in the software receiver, the DIF data affected by scintillation is necessary. Since such a data taken onboard is not available currently, the DIF is simulated for this research. For signal simulation purposes a device called a Digitized Intermediate Frequency Signal Generator ReGen from iP-Solutions is used. The DIF Signal Generator can create a DIF signal virtually indistinguishable from those which are recorded from live satellites. It also allows us to modify signal environment, introduce special errors, such as scintillation and modify error models. The phase and amplitude variation due to scintillation can be simulated by using appropriate shaping filters and probability distribution fitting [10]. However, the real phase/amplitude variation profiles associated with plasma bubble, which is partly shown in Fig.13, are used in this paper. First, a trajectory of a light aircraft and INS data are generated, and then corresponding GPS DIF data including scintillation effect is generated. Fig. 17 and Fig. 18 show the simulated flight profile and velocity of aircraft (NED) which is used for computing Doppler frequency. The aircraft took off and made one and half counter-clockwise rotations. Fig. 19 shows the variation of intensity and phase embedded in the DIF data, which corresponds to the beginning of scintillation (from 12h43m to 12h47m24s).

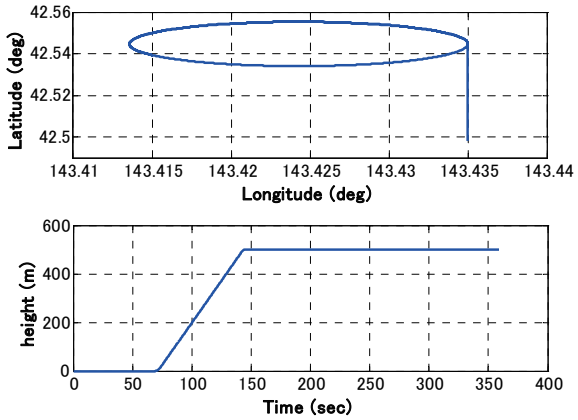

Figure 17 Simulated flight profile

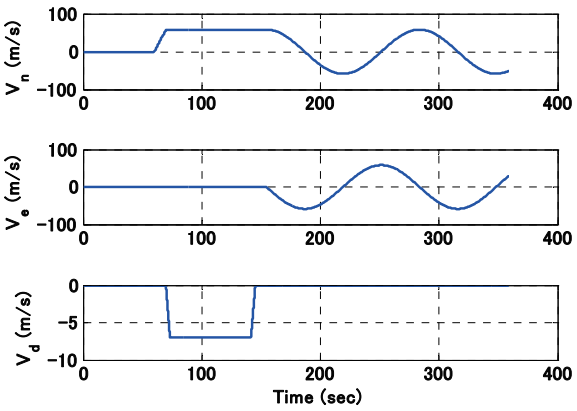

Figure 18 Velocity of aircraft (NED)

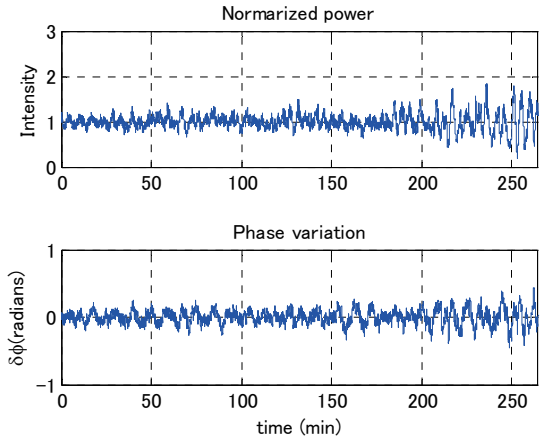

Figure 19 Intensity/phase variation used for simulation

4.2 Testing of Doppler Aiding

The carrier phase errors of eight satellites are shown in Fig. 20 where Doppler aiding is not applied. The scintillation effect is added on the signal of PRN15 after 90 seconds

from the time origin. The noise bandwidth was set at 12 Hz. It is clearly seen that the carrier error increases due to the scintillation. (Note that the vertical scales are different between PRN15 and other satellites.) Fig. 21 shows the carrier errors when Doppler aiding is applied. Comparing Fig. 20 and Fig.21, carrier error trends due to aircraft dynamics can be seen in Fig. 20. The standard deviations of carrier error (shown in figures) are reduced generally by applying Doppler aiding. However, cycle slips occurred frequently on PRN 15 even with aiding since the scintillation applied to this test was considerably strong. The effect of amplitude scintillation is clearly seen in Fig. 22, in which an example of I-channel amplitude for PRN 15 (time from 346 to 350 seconds) is depicted.

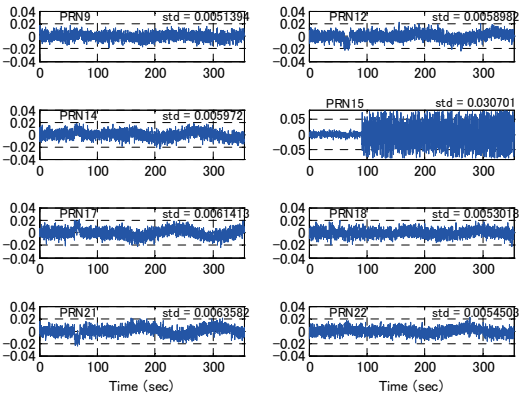

Figure 20 Carrier error for eight satellites with scintillation on PRN 15 (without aiding)

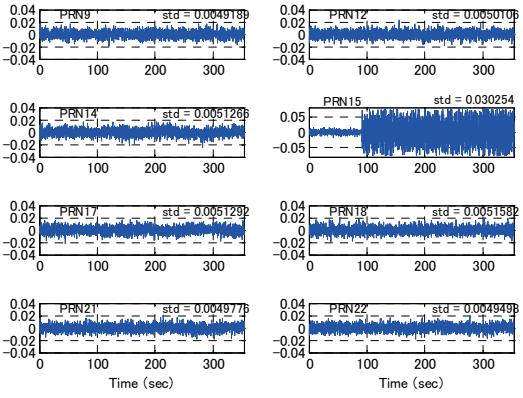

Figure 21 Carrier error for eight satellites with scintillation on PRN 15 (with aiding)

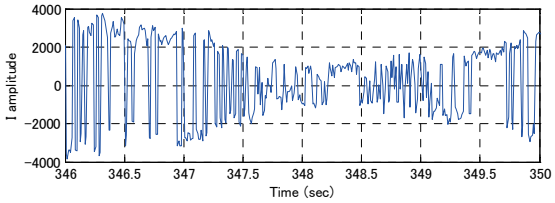

Figure 22 I-channel amplitude of PRN 15 (time from 346 to 350 seconds)

5. SUMMARY

A preliminary test of INS-aided GPS tracking loop performance under simulated ionosphere scintillation was conducted and described in this paper. Since flight test data under scintillation was not available at this stage, the DIF was simulated for the use of software receiver. The real data of scintillation associated with plasma bubble, which was observed at south Japan, was analyzed and extracted intensity/phase variation were embedded in the simulated DIF data. The improvement of carrier tracking by Doppler aiding was observed. However, the scintillation applied to this test was considerably strong and cycle slips occurred frequently even with aiding. Refinement of the tracking algorithms as well as power/noise adjustment of signal generator might be necessary. Also, the function of generating arbitrary scintillation is under development. Future work will include the implementation of Global Ionospheric Scintillation model [11], and this test extension will makes it possible to demonstrate an improved continuity/availability of precision approach under such severe environment.

6. ACKNOWLEDGMENTS

The authors would like to acknowledge the NICT Space Environment Group for providing TEC data at Taiwan.

7. REFERENCES

[1] AIP (Aeronautical Information Publication) Japan, ENR 4.2 Special navigation systems, Civil Aviation Bureau, Ministry of Land, Infrastructure and Transportation.

[2] T. Yoshihara, et. al., “Development of GBAS (Ground-Based Augmentation System) prototype for safety design and evaluation”, IEICE Technical Report SSS2010-3 (2010-05), The Institute of Electronics, Information and Communication Engineers. (in Japanese)

[3] T. Tsujii, T. Fujiwara, Y. Suganuma, H. Tomita, and I. Petrovski: Development of INS-aided GPS Tracking Loop and Preliminary Flight Test, *ICROS-SICE International Joint Conference 2009*, August 18-21, Fukuoka International Congress Center, Japan, pp.3585-3590, 2009.

[4] S. Saito, T. Yoshihara, and N. Fujii, "Study of Effects of the Plasma Bubble on GBAS by a Three-Dimensional Ionospheric Delay Model", 22nd International Technical Meeting of the Satellite Division of the Institute of Navigation, Sept. 22-25, 2009, Savannah, Georgia, US.

[5] S. Alban, D. Akos, S. Rock, and D. Gebre-Egziobher: Performance Analysis and Architectures for INS-Aided GPS tracking loops, *Proceedings of the ION National Technical Meeting*, Anaheim, CA, 22-24 January, pp.611-622, 2003.

[6] R. S. Conker, M. B. El-Arini, C. J. Hegarty, and T. Hsiao, "Modeling the Effects of Ionospheric Scintillation on GPS/SBAS Availability", Radio Science, Vol. 38, No. 1, January, 2003.

[7] Knight, M. F., Ionospheric Scintillation Effects on Global Positioning System Receivers, Ph.D. Thesis, The University of Adelaide, Adelaide, South Australia, December, 2000.

[8] T. Yoshihara, N. Fujii, K. Matsunaga, K. Hoshinoo, T. Sakai, and S. Wakabayashi, "Preliminary Analysis of Ionospheric Delay Variation Effect on GBAS due to Plasma Bubble at the Southern Region in Japan", Proc. of ION NTM 2007, pp.1065-1072, Jan. 2007, San Diego.

[9] A. J. Van Dierendonck and Q. Hua, Measuring Ionospheric Scintillation Effects from. GPS Signals, ION 57th Annual Meeting/CIGTF 20th Biennial Guidance. Test Symposium, 11-13 June 2001, Albuquerque, NM. Pp.391-396.

[10] Pullen, S., G. Opshaug, A. Hansen, T. Walter, P. Enge, and B. Parkinson, A preliminary study of the effect of ionospheric scintillation on WAAS user availability in equatorial regions, in Proc. of ION 1998, Inst, of Navigation., Alexandria, Va., 1998

[11] Beniguel, "Global Ionospheric Propagation Model (GIM): a propagation model for scintillation of transmitted signals", *Radio Sci.*, May 2002.

8. COPYRIGHT